ACS Catalysis

Research Article

pubs.acs.org/acscatalysis

Role of Au in Graphene Growth on a Ni Surface

Yucheng Huang,* Jinyan Du, Tao Zhou, Chongyi Ling, Sufan Wang, and Baoyou Geng

Center for Nano Science and Technology, College of Chemistry and Material Science, The Key Laboratory of Functional Molecular Solids, Ministry of Education, Anhui Normal University, Wuhu, 241000, People's Republic of China

Supporting Information

ABSTRACT: Density functional calculations were performed to investigate the role of Au in graphene growth on the Ni(111) step. It was shown that armchair (AC) and zigzag (ZZ) graphene edge growths have nucleation selectivity, depending on the curvature of the stepped surface. The AC and ZZ pristine graphene edges are energetically more favorable than the Ni-terminated one, and the stabilities of Au-passivated graphene edges strongly depend on the Au concentration. Au modification on the Ni terrace lowers the energy barrier of C incorporation onto the AC/ZZ graphene edge process, in agreement with the experimental observation that graphene can be produced at the low temperature of ~723 K with Au alloying. The growth rate of the AC graphene edge is always faster than the ZZ, leading to the ZZ edge's dominating the circumference of the growing graphene islands. With a decrease in the temperature, the increase in the AC graphene edge growth ratio greatly exceeds that of ZZ, driving the edges to incorporate a zigzag geometry. The overwhelming domination of ZZ edge rationalizes the experimental observation that Au modification can dramatically increase the quality of the graphene films at the lower temperature. On the basis of these results, we suggest that to obtain a high-quality graphene sheet on a Ni surface, the presence of a step should be necessary, and a promoter such as Au should be added to the Ni surface after graphene nucleation at the step edge site. Furthermore, this work not only provides implications on how to synthesize a high-quality graphene by a CVD approach but also guides inhibition of the undesirable graphene formation in some instances. This work represents the first attempt to investigate the graphene growth mechanism on a surface alloy by theoretical means, which will stimulate further experimental efforts to synthesize high-quality graphene by using a surface alloy as the substrate, especially the choice of an alloyed metal with low cost.

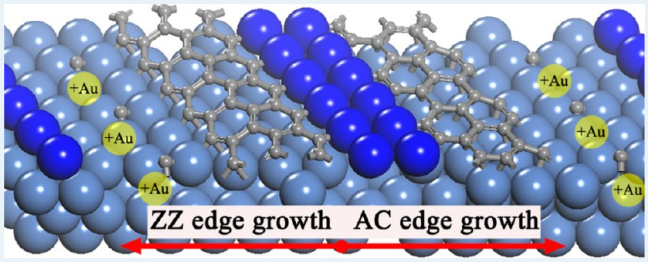

KEYWORDS: *Au/Ni alloy, high-quality graphene, density functional theory, carbon deposits, zigzag edge, growth mechanism*

INTRODUCTION

Because of its unique electrical, mechanical, and optical properties, graphene has attracted extensive research interest. The versatile properties of graphene endow its numerous potential applications in transistors, chemical and biosensors, energy storage devices, electromechanical systems, etc.[1] On the other hand, in some cases, the formation of graphene is undesirable. For example, in the course of hydrocarbon or alcohol steam reforming, the deposited carbon in the form of graphene would eventually deactivate the Ni catalysts, leading to low catalytic efficiency and high cost.[2,3] Thus, understanding the growth mechanism of graphene is of pivotal importance for the controllable synthesis of graphene and optimizing reaction conditions.

To realize the industrial applications, various experimental techniques have been applied to synthesize high-quality graphene in a large area, including mechanical peeling,[4] high-temperature sublimation of SiC,[5] reduction of graphene oxide,[6] and chemical vapor deposition (CVD),[7−13] among which CVD growth catalyzed by transition metal surfaces is the most promising. It has been demonstrated that numerous transition metals[7−13] can be used as the catalysts for graphene CVD epitaxial growth. Owing to a good match between the neighboring Ni−Ni interatomic distance and the lattice parameter of graphite, the Ni(111) surface is considered one of the most suitable candidates.[11] It was proposed that graphene growth on Ni surfaces is initiated from C atom segregation or precipitation, followed by graphene nucleation occurring at defects, such as step edges on the Ni surface. Finally, the small graphene flakes increase in size with the addition of C at the flake edges.

Recent theoretical efforts have focused mainly on the graphene nucleation process.[9,14−23] Since the diffusion barrier of C atoms is very low,[24] graphene growth should be limited by incorporating carbon atoms onto the edges of graphene islands. However, few have paid attention to how C atoms incorporate into the front of graphene and the growth mechanism. Shu et al.[25] reported the edge stability and kinetics of graphene CVD growth on the Cu(111) surface by density functional theory (DFT) calculations and concluded that Cu passivation on the armchair-like sites at the edge significantly lowers the barriers of incorporating C atoms onto the graphene edge, leading to the

Received: December 1, 2013
Revised: January 10, 2014
Published: February 4, 2014

   dx.doi.org/10.1021/cs401135g | ACS Catal. 2014, 4, 892−902

zigzag edges dominating the edge type of growing graphene islands. Wang et al.[26] investigated the formation and healing of vacancies in graphene CVD growth on Cu(111), Ni(111), and Co(0001) surfaces and found that Cu is a better catalyst than Ni for the synthesis of high-quality graphene in that the defects in the formed graphene on Cu are lower in concentration and can be more efficiently healed at the typical experimental temperature.

All the above studies are about monometallic catalysts and do not involve alloy systems. In fact, to resist the formation of the deposited carbon on the Ni surface during hydrocarbon or alcohol steam reforming, many methods have been used,[27−33] and one of them is the addition of precious metal to form the surface alloy, that is, AuNi, etc.[28] The improved thermal stability of the catalyst has been verified by much research, and a consensus was reached that the additives always block the step edge site. On the other hand, from the point of view of graphene synthesis, the blocking would decrease the quantity of formed graphene because graphene formation also occurs at the step edge site, which was supported by the work of Weatherup et al. concerning a Au-modified Ni surface.[34] Different from the typical CVD temperature of 1200 K, a much lower temperature, ∼ 450 °C, was reported able to make a high-quality graphene synthesis possible.[34] Actually, because of better performance than monometallic catalysts (quality not quantity), recently, experimentalists have been extensively working on alloy catalysts of metal−nickel, such as Au−Ni,[34] Cu−Ni,[35,36] and Ni−Mo,[37] etc., for graphene CVD epitaxial growth.

Needless to say, the atomic level mechanism of C atoms incorporating onto an edge of a graphene sheet, which is difficult to access by current experimental techniques, would undoubtedly help us better understand the growth process, and knowledge about graphene growth on metal surfaces, especially alloy surfaces/surface alloys, can guide us both to synthesize high-quality graphene and to inhibit carbon deposits for extending the lifetime of catalysts. Considering there are few papers dealing with alloy systems, herein, we give a full account of our theoretical investigations toward the role of Au in graphene growth on a Ni surface. Using first-principles calculations, we examined the role of Au in graphene growth on a Ni surface. Importantly, our results showed that during a round of edge formation, Au addition on a Ni terrace lowers the energy barriers of C incorporation onto the front of graphene. Since added Au preferentially blocks the step edge site on the Ni surface and thereby suppresses the formation of graphene, our results suggest that a high-quality graphene sheet might be obtained by addition of Au after graphene nucleation. Moreover, kinetic analysis demonstrates that the zigzag graphene edge would dominate the circumference of growing graphene islands, and this dominance will become more remarkable at lower temperature because the armchair graphene edge grows faster, driving the edges to be in a zigzag geometry. Overall, our results not only provide a rational basis for understanding recent experimental observations[34] but also shed light on synthesizing high-quality graphene by the CVD approach as well as preventing the formation of graphene in some instances.

METHODS AND MODELS

All spin-polarized calculations were preformed by using the density functional theory (DFT) as implemented by the Vienna Ab Initio Simulation Package (VASP).[38−40] The exchange-correlation energy was described in the generalized gradient approximation (GGA) using the Perdew−Burke−Ernzerhof (PBE)[41] functional. The energy cutoff of the plane-wave expansion was set to 400 eV using the projector-augmented wave (PAW)[42,43] potentials to describe the electron−ion interaction. Conjugated gradient atomic optimization was performed with a criterion of convergence of 0.02 eV/Å. A 1 × 3 × 1 Monkhorst−Pack k-point mesh[44] was chosen in the Brillouin zone integration with the Methfessel−Paxton method,[45] which can give the results of <5 kJ/mol difference with that calculated by denser k-point sampling (Table S1 in the Supporting Information (SI)). The climbing image nudged elastic band (CI-NEB) method[46,47] was used for the transition state search. Each transition state was verified by vibrational mode analysis, confirming a unique normal mode eigenvector corresponding to negative curvature at saddle point.

It is well-known that graphene growth tends to begin at the metal step for most metal surfaces. Previous studies used (211) and (321) surfaces to model the metal step.[22] In view of higher surface energies, here, a three-layer slab of Ni(111) with (2 × 8) surface unit cells was used to represent the metal surfaces, and then a (2 × 2) Ni stripe was added to mimic the Ni(111) step (Figure 1). This kind of model was proved to be appropriate to represent the graphene growth near a metal step.[25,48] The bottom layer was fixed throughout the calculations. Graphene with two kinds of edges, armchair (AC) and zigzag (ZZ), was anchored on the Ni(111) step to model the growing graphene. Another edge was used to represent the growing front of graphene which is active for the incorporation of C atoms. For the model of a Au-modified Ni(111) step, we put the Au atoms into the Ni terrace. This is based on two considerations: First, the role of Au at the step edge on the graphene growth is extremely clear, namely, it would resist the formation of graphene because both graphene nucleation and Au blocking preferably occur at the step edge site. Second, the migration of Au from step to terrace on the Ni surface is more favorable than that of Ni (SI Figure S1). At high temperature under CVD experimental conditions, Au is more likely to be thermally activated on the Ni surface.

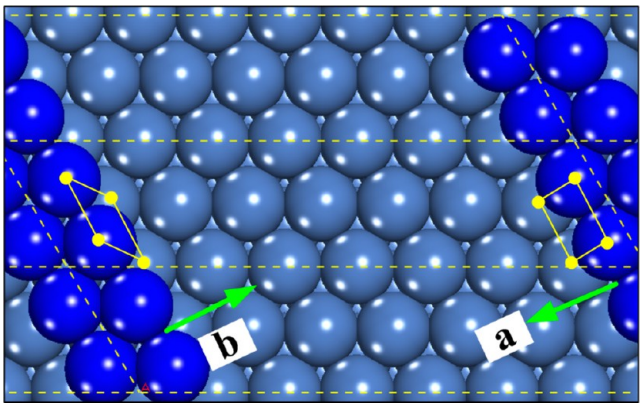

Figure 1. The model of the Ni(111) step. Two rows of Ni stripes are highlighted with blue. a, b denotes two growth directions for graphene. The initial C atom can be adsorbed on either a position of a parallelogram or a rectangle site (yellow solid lines). The surface unit cells are shown with yellow dashed parallelograms.

RESULTS AND DISCUSSION

3.1. Stability of Graphene on the Pure and Au-Modified Ni(111) Steps. When a (2 × 2) Ni stripe is added

dx.doi.org/10.1021/cs401135g | ACS Catal. 2014, 4, 892−902

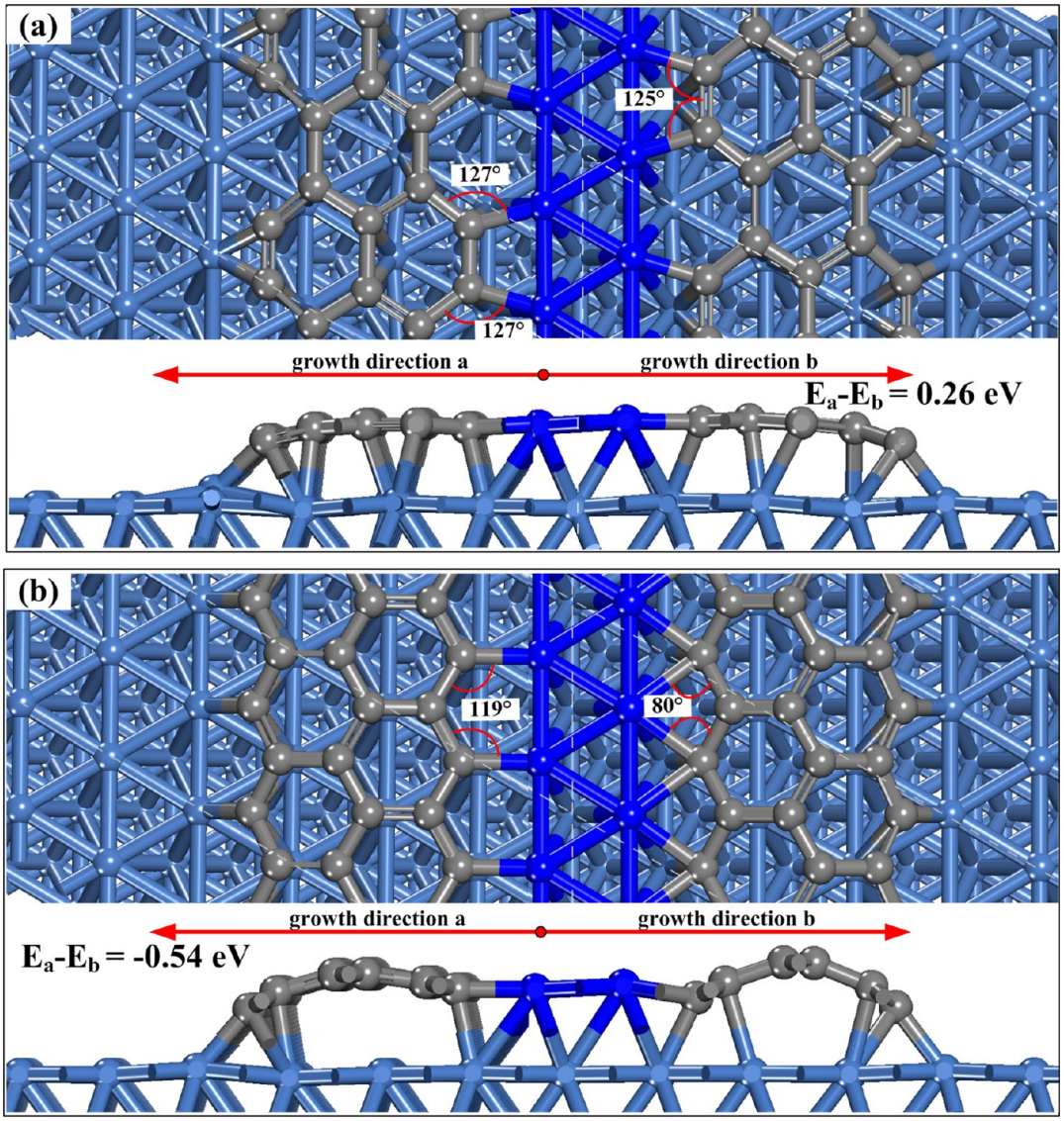

Figure 2. (a) AC and (b) ZZ graphene edge growth initiate at the step edge on Ni(111) step. E_a/E_b denotes the formation energy of graphene on the Ni(111) step. The stepped Ni atoms are highlighted with blue.

on the Ni(111) surface, two kinds of step edges with different curvature are thereby produced. Obviously, the initial C atom can be adsorbed on either a position of a parallelogram or a rectangle site (Figure 1). Accordingly, graphene growth can be initiated from the direction of either a or b (Figure 1). As indicated below, graphene with different edge shapes prefers different growth directions. Calculations show that AC edges tend to grow from the direction of b, and ZZ ones prefer the direction of a, which can be rationalized with the deviation of the C−C−Ni angle from 120°. It can be seen in Figure 2a that for the AC edge, the C−C−Ni bond angle of the *b* direction is closer to the standard sp^2 bond angle in graphene (120°) than that of the *a* direction. Hence, the *b* direction is more suitable for AC graphene edge growth. In contrast, the C−C−Ni bond angle in the *b* direction for the ZZ edge, 80°, differs significantly from the standard angle, but along the *a* direction, the C−C−Ni, 119°, is very similar to 120°, indicating that the ZZ edge should preferably grow from the *a* direction (Figure 2b). Note that this kind of chirality selectivity was also observed by Balbuena et al.,[22] who found that the Co(211) surface prefers ZZ graphene formation, and Co(321) prefers AC. Importantly, our observations can shed light on understanding the experimental findings that the dominant edge type of the grown graphene islands on the transition metal surfaces is always ZZ.[49] On one hand, because of the nice match of the C−C−Ni angle to the standard 120°, favorable growth in the ZZ mode can be expected. On the other hand, graphene growth has nucleation selectivity; that is, AC and ZZ edges separately nucleate from each preferable direction. In the following paragraph, we will show that the growth rates of the AC edge always overwhelm that of the ZZ. On the basis of the crystal growth theory that the faster growing edges would quickly disappear,[50] thus, the final dominating edge is ZZ.

Recent work showed a Cu-terminated AC edge is energetically more preferable than a pristine one on the Cu(111) surface.[25] To verify whether the pristine graphene edges are favorably terminated by thermally activated metal atoms, four types of Ni-terminated graphene edges on Ni(111) were exploited in the present study (Figure 3b, c, g, h). In addition, another four types of Au-terminated edges were also investigated to probe the role of Au in graphene growth (Figure 3d, e, i, j). Reference systems of pristine AC and ZZ

dx.doi.org/10.1021/cs401135g | *ACS Catal.* 2014, 4, 892−902

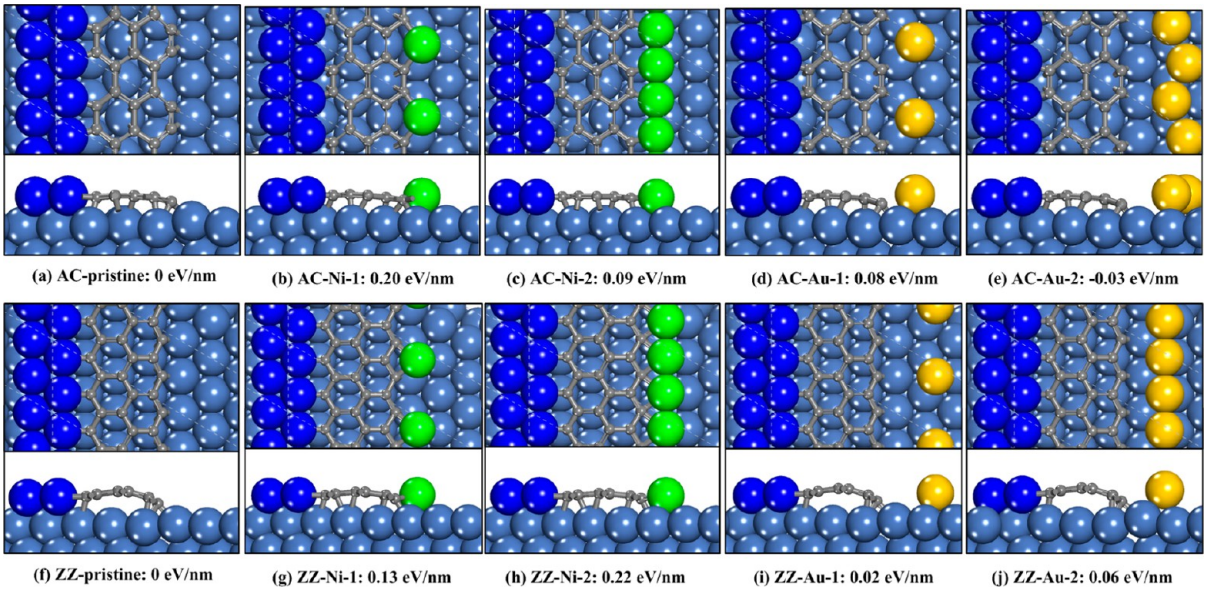

Figure 3. Top and side views of the AC and ZZ graphene edge configurations on Ni(111) steps. The relative formation energies of each structure relative to the pristine AC/ZZ edge are shown. (a, f) Pristine AC/ZZ graphene edge; (b, g) AC/ZZ graphene edges terminated by an isolated Ni atom (labeled as AC-Ni-1/ZZ-Ni-1); (c, h) AC/ZZ graphene edges terminated by a linear Ni chain (labeled as AC-Ni-1/ZZ-Ni-2); (d, i) AC/ZZ graphene edges terminated by an isolated Au atom (labeled as AC-Au-1/ZZ-Au-1); and (e, j) AC/ZZ graphene edges terminated by a linear Au chain (labeled as AC-Au-1/ZZ-Au-2). The stepped Ni and terminated Ni/Au are highlighted with blue and green/yellow, respectively.

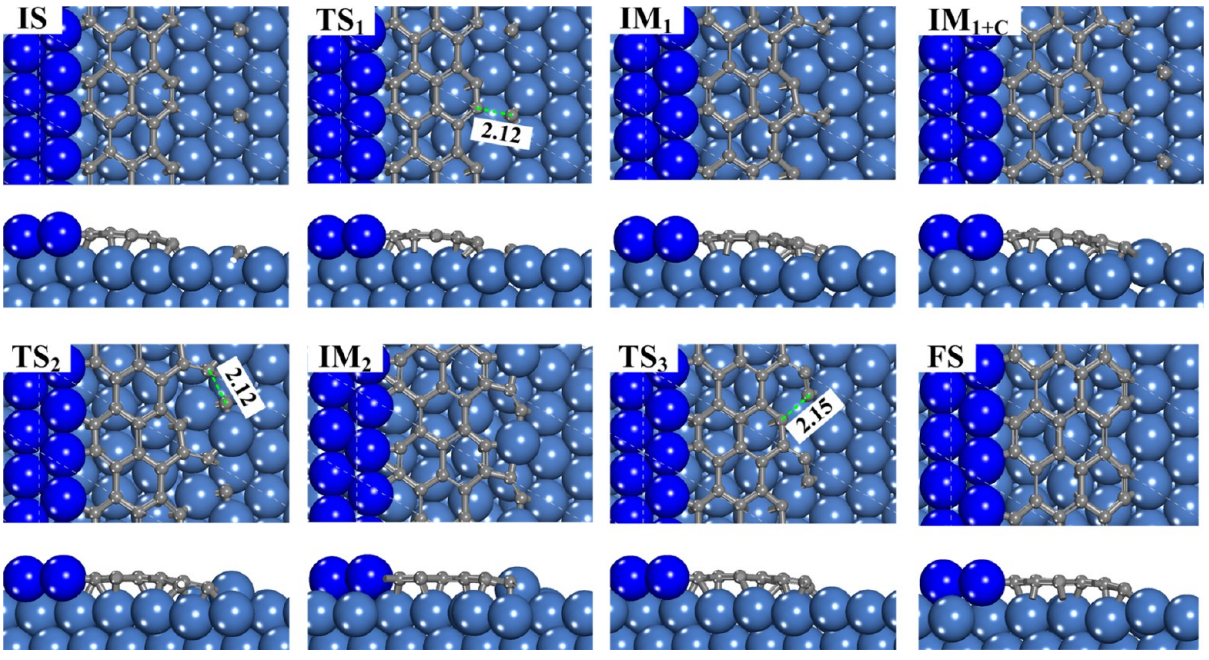

Figure 4. Top and side views of the structures (ISs, TSs, and FSs) during a repeatable cycle of incorporating two C atoms onto pristine AC graphene edges on a Ni(111) step. C−C distances in each TS are labeled in Å.

edges are showed in Figure 3a and f, respectively. The formation energies (E_f) of Ni/Au-terminated graphene edges, are defined as:[25] $E_f = (E_T - E_G - E_s - N_{Ni/Au} \times \varepsilon_{Ni/Au})/L$, where E_T, E_G, and E_S are the energies of the graphene on the Ni surface, graphene is in the gas state, and the Ni substrate, respectively; $\varepsilon_{Ni/Au}$ is the cohesive energy of the Ni/Au bulk in eV/atom; $N_{Ni/Au}$ is the number of terminating Ni/Au atoms; and L is the length of the graphene edge. For pristine graphene edges, E_f is defined as: $E_f = (E_T - E_G - E_s)/L$. As shown in Figure 3, the Ni-terminated graphene edges are less stable than the pristine ones. Thus, graphene can favorably grow without the aid of activated Ni atoms on the Ni(111) step. At variance, the stabilities of Au-terminated graphene edges strongly depend on the Au concentrations. For one Au atom passivation, the formation energies are slightly higher than the pristine one; however, when Au atoms are lined on the front of graphene growth edge, the formation energies are somewhat lower than on the pristine one due to more Au−Au bonding. Obviously, once the Au line is formed on the Ni surface, it acts as a "riverbank" to block graphene growth. Thus, there is no doubt that excessive addition of Au would hamper the formation of

dx.doi.org/10.1021/cs401135g | ACS Catal. 2014, 4, 892−902

Table 1. Reaction Heats and Activation Energies (in eV) of AC/ZZ Graphene Edge Growth on Ni(111) Step with and without the Addition of Au[a]

AC edge growth	E_a	ΔH	ZZ edge growth	E_a	ΔH
$R_1(R_1')$: $IS^{(Au)} \xrightarrow{TS_1^{(Au)}} IM_1^{(Au)}$	0.96 (0.99)	−0.07 (−0.21)	$R_1(R_1')$: $IS^{(Au)} \xrightarrow{TS_1^{(Au)}} IM_1^{(Au)}$	0.73 (0.65)	−0.14 (−0.26)
$R_{21}(R_{21}')$: $IM_{1+C}{}^{(Au)} \xrightarrow{TS_2^{(Au)}} IM_2^{(Au)}$	1.54 (1.28)	−0.33 (−0.87)	$R_{21}(R_{21}')$: $IM_{1+C}{}^{(Au)} \xrightarrow{TS_2^{(Au)}} IM_2^{(Au)}$	1.63 (1.61)	−1.09 (−1.14)
$R_{22}(R_{22}')$: $IM_2{}^{(Au)} \xrightarrow{TS_3^{(Au)}} FS^{(Au)}$	0.60 (0.91)	−0.70 (−0.41)	$R_{22}(R_{22}')$: $IM_2{}^{(Au)} \xrightarrow{TS_3^{(Au)}} IM_3^{(Au)}$	1.05 (0.57)	0.21 (−0.11)
			$R_{31}(R_{31}')$: $IM_{3+C}{}^{(Au)} \xrightarrow{TS_4^{(Au)}} IM_4^{(Au)}$	0.85 (0.57)	−0.78 (−1.06)
			$R_{32}(R_{32}')$: $IM_4{}^{(Au)} \xrightarrow{TS_5^{(Au)}} IM_5^{(Au)}$	2.12 (2.24)	−0.10 (0.76)
			$R_4(R_4')$: $IM_{5+C}{}^{(Au)} \xrightarrow{TS_6^{(Au)}} FS^{(Au)}$	2.64 (1.26)	−2.37 (−3.74)

[a]The values in parentheses are the corresponding ones on Ni(111) step with Au modification.

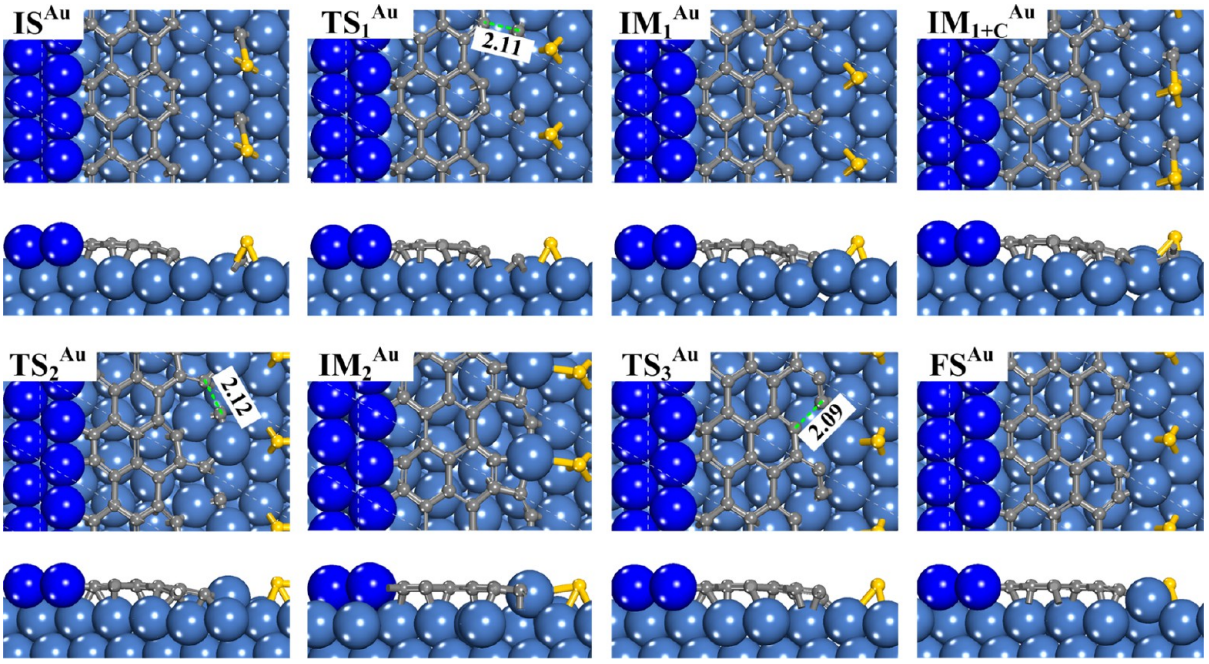

Figure 5. Top and side views of the structures (ISs, TSs, and FSs) during a repeatable cycle of incorporating two C atoms onto Au-terminated AC graphene edges on Ni(111) step. C−C distances in each TS are labeled in Å.

graphene. In the following, we discuss only isolated Au atoms presented in the graphene growth front.

3.2. Reaction Mechanisms of C Incorporation onto the Graphene Edge. *3.2.1. Repeated Cycles of Two C Atoms onto the Pristine AC Graphene Edge with or without the Presence of Au.* The reaction mechanism of C incorporation onto the pristine AC graphene edge is first addressed as a reference. Here, Ni-terminated AC/ZZ growth was not considered because (i) the termination of Ni notably decreases the stability of graphene, (ii) the diffusion barrier of a Ni adatom is higher than that of Au because the Ni−Ni bond bonding is stronger than Ni−Au (SI Figure S1). In Figure 4, the detailed processes of incorporating C atoms onto AC edges on pure Ni surfaces are illustrated, where we consider only a C monomer incorporating because very recent first-principles calculations have proposed that incorporation of a C dimer takes place when the C−metal interaction is weak,[16] which is not the present case.

Difficult incorporation of C dimers and trimers is also supported by molecular dynamic simulation, which has shown that the diffusion barriers of C dimers or trimers are quite large, resulting in dramatically hampered diffusion and coalescence of C atoms on the Ni(111) surface.[17] Provided a source C atom located on a hollow site adjacent to the pristine AC edge on Ni(111) terrace acts as the initial state (IS), the incorporating reaction begins (Figure 4). Undergoing a transition state (TS_1) with the C−C distance shrunk to 2.12 Å, an intermediate (IM) named IM_1 with a C−C dangling bond was generated. This structure was proved to be highly stable when it is formed on a Ni(111) planar surface.[48] In contrast, on a Ni(111) step, the formation energy of IM_1 is not the lowest (it is 0.2 eV higher than that of the pristine graphene), showing that graphene nucleation on the step greatly stabilizes the AC edge, in agreement with a wide range of experimental observations.[7,15]

In addition to the different initial growth site, the different curvature of the bent graphene between those formed on facets and the one on steps should also affect the edge formation

dx.doi.org/10.1021/cs401135g | ACS Catal. 2014, 4, 892−902

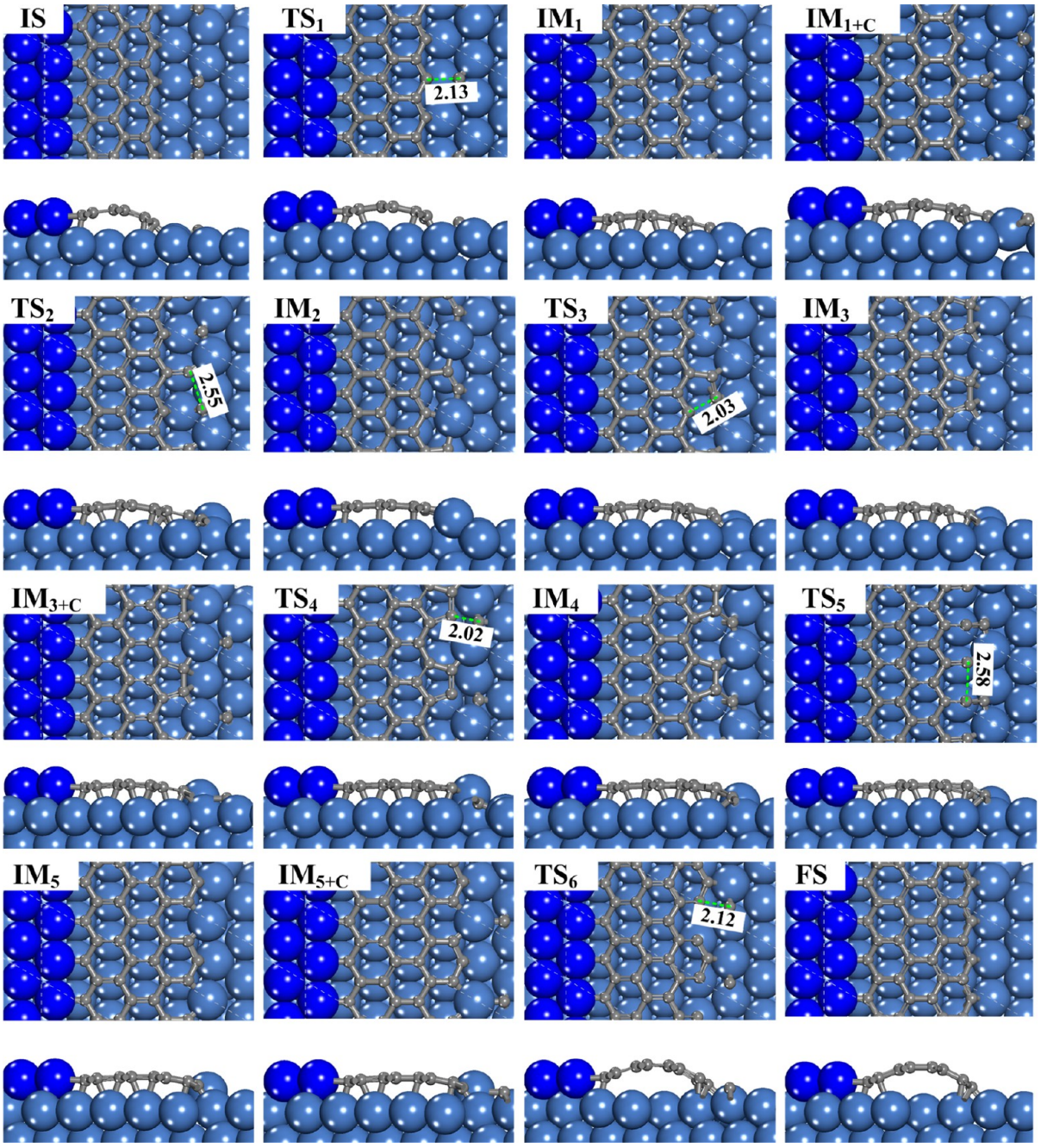

Figure 6. Top and side views of the structures (ISs, TSs and FSs) during a repeatable cycle of incorporating four C atoms onto pristine ZZ graphene edges on the Ni(111) step. C−C distances in each TS are labeled in Å.

energy. The first C addition step needs to overcome an energy barrier of 0.96 eV. This step is essentially thermoneutral (Table 1). To accomplish one cycle of AC edge growth, another C atom should be added to the edge. Interestingly, the second C incorporating process needs to experience TS_2 to obtain an intermediate of IM_2, and then the FS can be ultimately formed.

The threshold step of the second C addition is the production of the IM_2 with an energy barrier of 1.54 eV, in which one Ni atom is drawn out from the Ni(111) surface, leading to the formation of so-called BM (bridged metal) C−Ni−C structures. The formation of the BM structure is exothermic by 0.33 eV, indicating that the structure of IM_2 is relatively stable. Wu et al. demonstrated that BM structures can be spontaneously formed on Cu, Ag, and Ni(111) surfaces.[51] It is worth noting that our obtained growth mechanism does not involve a C pentamer, which is different from that on the Cu(111) surface.[23] To confirm the absence of pentamer during an AC edge growth cycle, the potential formation channel of a C pentamer from IM_1 was carefully examined, as shown in SI Figure S2. Calculations show that the reaction has an energy barrier of 1.13 eV with a high endothermicity of 1.04 eV. Thus, the reverse reaction has an energy barrier of only 0.1 eV, indicating that even if a pentamer is formed, it is very easy to reconstruct to the structure of IM_2.

With the modification of Au, accomplishing one AC edge growth cycle experiences the same process as on Ni(111) step. As illustrated in the states of IS^{Au}, IM_{1+C}^{Au} and IM_2^{Au} (ISs of each elementary step, Figure 5), Au has bonded to the additive C

dx.doi.org/10.1021/cs401135g | ACS Catal. 2014, 4, 892−902

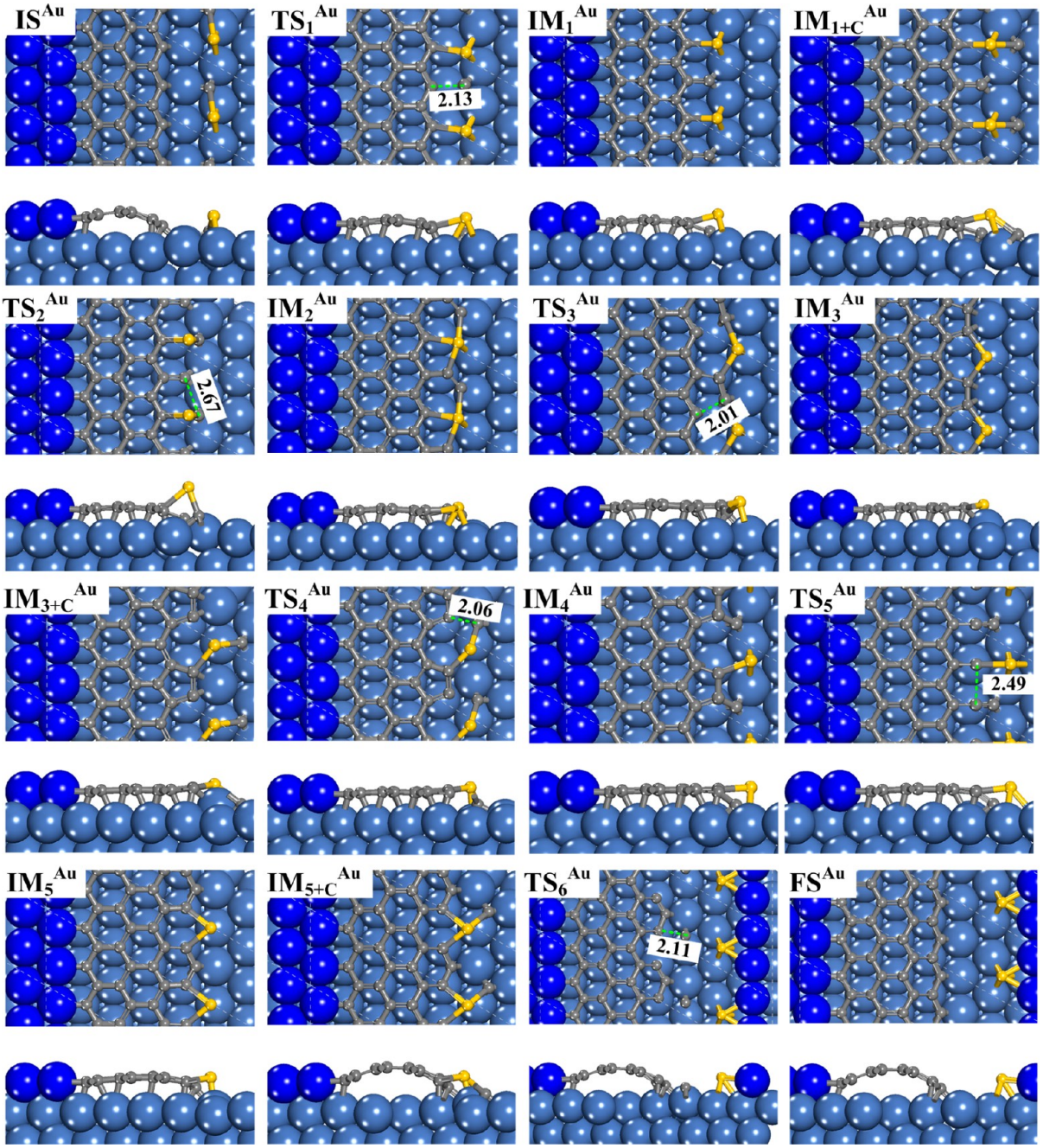

Figure 7. Top and side views of the structures (ISs, TSs, and FSs) during a repeatable cycle of incorporating four C atoms onto Au-terminated ZZ graphene edges on the Ni(111) step. C−C distances in each TS are labeled in Å.

atom, indicating that Au does participate the reaction; however, in the remaining states, Au acts more as a "standby" because Au is always far from the reaction center. The role of Au can be thereby summarized from two respects. First, it affects the stability of the graphenic C cluster in IS^{Au} and IM_{1+C}^{Au}. In each C-introducing process, the source C binds to an Au atom, resulting in destabilization of the initial states. It was evidenced by comparing the formation energies of the C cluster between IS and IS^{Au} as well as IM_{1+C} and IM_{1+C}^{Au}, both increasing by 0.08 eV/Å. On the other hand, Au has little effect on the stability of its corresponding TSs. Accordingly, these two elementary reactions become more preferable with the Au modification. Second, the BM structure also appears in IM_2^{Au} as seen in IM_2; however, the additional interaction between Au and the bridged Ni (denoted hereafter as Ni_b) presented in IM_2^{Au} enhances its stability (the formation energy of C clusters decreases by 0.04 eV from IM_2 to IM_2^{Au}), leading to the increase in the reaction barrier from $IM_2{}^{Au}$ to FS compared with the one on Au-free surfaces. To summarize, Au addition decreases the stability of IS without the BM structure, while it enhances the stability of IS with the BM structure. Counting the number of chemical bonds with Au, one can find that there are one Au−C and three Au−Ni bonds in IM_{1+C}^{Au} and four Au−Ni bonds, including one Au−Ni_b, present in IM_2^{Au}. Because both Au atoms adsorb at the 3-fold hollow site (Figure 5), the binding strength with the terrace is evaluated to be essentially identical, and thus, the different role of Au on BM and no-BM structures can be

dx.doi.org/10.1021/cs401135g | ACS Catal. 2014, 4, 892−902

rationalized by the bonding competition between Au−C and Au−Ni_b interactions.

As shown in Table 1, with or without the presence of Au, the threshold step of the whole growth cycle is the formation of IM_2/IM_2^{Au}, and the corresponding energy barrier reaches 1.54/1.28 eV on Au-free/Au-passivated Ni(111) step. Obviously, the presence of Au facilitates AC graphene edge growth.

3.2.2. Repeated Cycles of Four C Atoms onto the Pristine ZZ Graphene Edge with or without the Presence of Au. To finish a round of ZZ edge growth, four C atoms should be added to the graphene edge. Our calculations show that the whole growth process not only just simply experiences four elementary reactions, but also needs to undergo two additional steps involving the structures, such as BM and pentamer intermediates. Figures 6 and 7 illustrate the structures of IS, TSs, IMs, and FS along each reaction channel for one ZZ edge growth cycle with or without the presence of Au. Both have six elementary steps in total.

For a pristine ZZ graphene edge, the first C embedding initiates from the source C atom approaching the edge. When the C−C bond decreases to 2.13 Å, the TS_1 is formed. This process needs to surmount an activation energy of 0.73 exhibiting a reaction heat of −0.14 eV. Just like what we have found for the AC edge growth, the second C addition is a two-step process: an intermediate of IM_2 with the BM structure is produced first, and then it reconstructs to IM_3 with a C pentamer ring. From IM_2 to IM_3, the bridged Ni atom in IM_2 goes back to its original position in IM_3; meanwhile, another bridged Ni atom appears, forming a six-membered ring of C_5Ni adjacent to the C pentamer. The formation of IM_2 is exothermic by 1.09 eV. The formation of IM_3 is endothermic by 0.21 eV, indicating that the structure of IM_2 is more stable than IM_3. The threshold step of the second C embedding is the formation of IM_2 with a barrier of 1.63 eV (Table 1). Subsequently, the third C incorporation also experiences a two-step reaction: namely, the C atom first attaches to the C pentamer by forming a C−C dangling bond in IM_4, and then the healing of the pentamer can be achieved by rotating the dangling C−C bond. The final state of this process is IM_5, which also exhibits the BM structure with two sp hybridization C atoms passivated by the bridged Ni atom. The formation of IM_5 is a rate-determined step (RDS) in the third C addition reaction, and the barrier is substantial, 2.12 eV. The high barrier of pentamer healing by C−C dangling bond rotating was also found by Shu et al. on the Cu(111) surface.[25] Finally, to accomplish a complete growth round of the ZZ edge, the fourth C incorporation is needed. As shown in Figure 6, when the C−C distance shrinks to 2.12 Å, the TS_6 is reached, and the corresponding barrier is as high as 2.64 eV. This step is strongly exothermic, with the reaction heat of −2.37 eV, reflecting the strong driving force to ultimately form the domelike graphene.

In analogy with the growth mechanism on pure Ni, a new round of ZZ graphene growth on a Au/Ni surface also has to experience six elementary steps. Interestingly, as depicted in Figure 7, Au addition extinguishes all the BM structures and thereby alters the whole kinetics of the growth process. The big difference from the AC edge growth is that the Au atom participates in bonding with the C in almost all the states. This phenomenon stems from the more reactive C atom from the ZZ edge, which has two unpaired electrons,[20] whereas the C atom of the AC edge has one dangling σ bond due to the self-passivation effect.[21] The charge density difference analysis provides more detailed information. As shown in Figure 8a and c, the charge of the AC graphene edge is distributed over the whole C system, while the charge of the ZZ edge is localized mainly on the edge site. The delocalized charge distribution of the AC edge is due to the C−Ni bonding, leading to the formed graphene being closer to the surface compared with the ZZ.

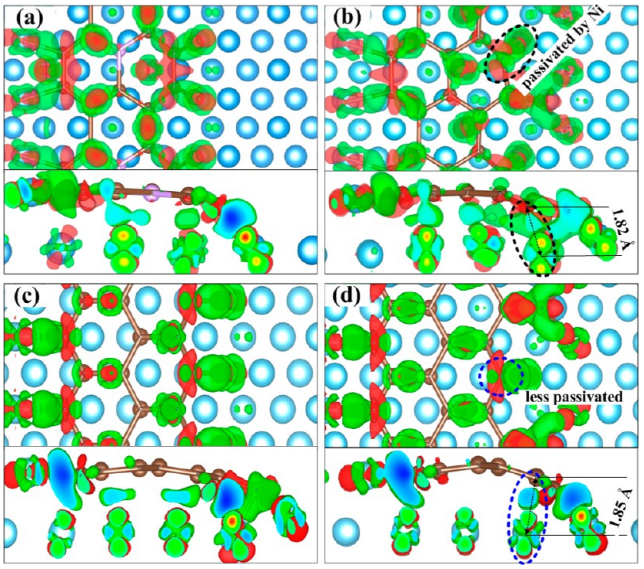

Figure 8. Top and side views of the charge density difference of (a) the pristine AC edge, (b) the AC edge with one C−C dangling bond (IM_1 in Figure 4), (c) the pristine ZZ edge, and (d) the ZZ edge with one C−C dangling bond (IM_1 in Figure 6). The red/blue regions represent charge depletion/accumulation, respectively. The isosurface value is set to be 0.008 eV/Å^3.

The self-passivation effect of C from the AC edge also appears during the C incorporation process. Taking IM_1 as an example, the sp hybridization C atom from the AC edge is more likely to be completely passivated by the surface Ni, resulting in less reactivity. In contrast, the C atom from the ZZ edge is less passivated by the surface Ni, which is evidenced by the fact that the C−Ni bond length is shorter than the corresponding one of the AC edge (Figure 8b and d). The more reactive C atom makes the edge C be terminated by Au and the surface Ni atom simultaneously, and thus, the Au atom is always favorably involved in the ZZ edge growth process.

Because of the interaction of C−Au, the Ni atom does not need to lift up from the surface to form the BM structure during the growth process. As discussed in Section 3.2.1, the formation of the BM structure enhances the stability of the IS, resulting in an increase in the energy barrier for C incorporation. Therefore, the absence of a BM structure on the Au modified Ni(111) step implies that the reaction barrier would no longer increase with respect to the one on the Au-free Ni(111) step. Indeed, as shown in Table 1, addition of Au lowers the energy barriers of almost all the elementary steps compared with the ones on Au-free surface, with the exception of R'_{32}. To understand the role of Au, all the structures on the Au-free surface were divided into two categories: one without the BM structures (IS, TS_1, IM_1, TS_3, IM_3, TS_6, and FS), the other with (the remaining ones). Au modification on those having no-BM structures does not notably alter their stabilities; in some cases, it even enhances them (e.g., for TS_3 and TS_6, the formation energy of the C cluster decreases with Au addition). On the other hand, Au modification on those with the BM structures reduces the stability of the structure. According to

dx.doi.org/10.1021/cs401135g | ACS Catal. 2014, 4, 892−902

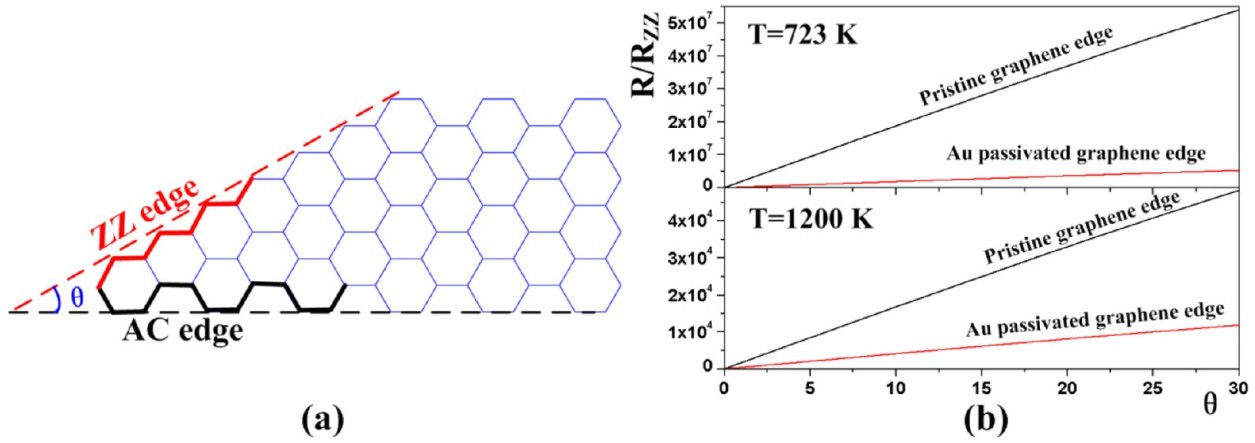

Figure 9. (a) Schematic illustration of an arbitrary graphene edge with the title angle θ, $0° \leq \theta \leq 30°$. (b) Ratio of growth rate (R/R_{ZZ}) of an arbitrary graphene edge as a function of θ.

this simple classification, R_1 belongs to the first type because both IS and TS have no BM structures; hence, Au modification produces an energy barrier nearly identical to the one on Au-free surface. R_{21}, R_{31}, and R_{32} belong to the second type because both IS and TS have BM structures; thereby, the energy barrier fluctuation depends on the relative alternation of the stability between IS and TS with Au addition: it always changes a little because the effect on the IS is close to the one on the TS. R_{22}, R_4 can be classified into the third type. In this type, the IS has BM and the TS has no BM structure (even so, Au can stabilize the TSs), leading to destabilization of the IS but stabilization of the TS, which eventually decreases the energy barrier. Generally, the IS without BM structure is more likely to be carbonated. This result will stimulate further experimental efforts to synthesize the high-quality graphene by using an alloy, especially to determine which kind of the alloyed metal with low cost can extinguish the BM structure during the process of graphene growth.

The RDS of the new round of ZZ edge growth is the step of the fourth C incorporation on the Au-free Ni(111) step while it turns to the formation of the IM_S^{Au} on Au modified step. The threshold barrier decreases by 0.40 eV as a result of the addition of Au, indicating introduction of Au also favors the formation of the ZZ graphene edge.

3.3. Growth Rate of Graphene Edge at Different Temperatures. The growth rate of an arbitrary graphene edge can be expressed as $R = R_{AC}\cdot c_{AC} + R_{ZZ}\cdot c_{ZZ}$, where R_{AC}/R_{ZZ} denotes the growth rate of the AC/ZZ edge, and c_{AC}/c_{ZZ} represents the concentrations of AC-/ZZ-like sites. It can also be defined as $R = (4/(3)^{1/2})\cdot R_{AC}\cdot\sin(\theta) + 2\cdot R_{ZZ}\cdot\sin(30 - \theta))$, where θ is the tilt angle of the arbitrary graphene edge from the AC direction (Figure 9a). The detailed formula derivation processes can be seen in ref 52. The ratio of R/R_{ZZ}, accordingly, can be written as $(R/R_{ZZ}) = ((4/(3)^{1/2})\cdot(R_{AC}/R_{ZZ})\cdot\sin(\theta) + 2\cdot\sin(30 - \theta) = (4/(3)^{1/2})\cdot\exp - ((E_{a,AC} - E_{a,ZZ})/RT)\cdot\sin(\theta) + 2\cdot\sin(30 - \theta))$. Here, the relationship of $R\infty \exp(-(E_a/RT))$ was used. $E_{a,AC}/E_{a,ZZ}$ denotes the threshold barrier of the AC/ZZ edge growth, R is the gas constant, and T is the temperature of graphene growth. Figure 9b shows the ratios of R/R_{ZZ} as a function of θ with or without the passivation of Au. Two temperatures were selected: one is the typical temperature of graphene CVD growth, T = 1200 K; the other is T = 723 K, which was proved to be sufficient for obtaining high-quality graphene films by using a Au−Ni alloy catalyst.[32] We have shown that the threshold barrier of incorporating C atoms onto a pristine ZZ edge is higher than onto a pristine AC edge, regardless of whether Au is present; thus, the growth rate monotonically increases with θ (Figure 9b). When θ takes an arbitrary value within the limits of 0 (corresponding to the AC edge) < $\theta \leq 30°$ (the ZZ edge), the value of R/R_{ZZ} is far greater than 1. As a consequence, slowly growing the ZZ edge should dominate the edge of the growing graphene islands according to the classical crystal growth theory.[50] As described, a graphene edge passivated by Au atoms lowers the threshold barrier of ZZ edge growth; thus, addition of Au would decrease the CVD temperature, which is in good agreement with the experimental results.[34] Another interesting finding is that with a decrease in the temperature, the slope of the functional relationship between R/R_{ZZ} and θ becomes larger, indicating that the AC edge growth is faster at 723 than at 1200 K. The rapid AC edge growth leads to its rapid disappearance; thus, the slowly grown ZZ edge absolutely dominates the circumference of a growing graphene island, which may be one of the reason why Au modification can induce a dramatic increase in the quality of graphene films.[34]

The results in this paper can give enlightenment to the synthesis of high-quality graphene, and also a means to resist the formation of graphene in some cases. The Ni step not only is the nucleation center for graphene but also directs the AC/ZZ graphene edge growth toward different directions. Therefore, the existence of a step can avoid the disorderly growth of graphene, which may be the basis for acquiring high-quality graphene. Au modification at the step site on the Ni surface hampers the formation of graphene; however, Au on the terrace lowers the energy barrier for incorporating C onto the graphene edge and accelerates the growth of the AC/ZZ graphene edge. On the basis of these findings, we suggest that to obtain a high-quality graphene sheet on a Ni surface, the presence of a step should be necessary, and a promoter such as Au should be added into the Ni surface after graphene nucleation at the step edge site.

CONCLUSIONS

In summary, we have performed a detailed theoretical investigation on the stability and growth kinetics of graphene edges on the Ni(111) step with and without the passivation of Au. Our results show that AC and ZZ graphene edge growths have nucleation selectivity, depending on the curvature of the

dx.doi.org/10.1021/cs401135g | ACS Catal. 2014, 4, 892−902

stepped surface. The presence of steps can avoid disorderly growth of graphene, which may be the basis for acquiring high-quality graphene. The Ni-terminated graphene edges are always less stable than pristine ones, and the stability of Au-terminated graphene edges strongly depends on the Au concentrations. Au modification on a Ni(111) step lowers the threshold barrier of AC/ZZ graphene edge growth, which is in fair agreement with the experimental observations that graphene films can be made at lower temperature with Au addition. The growth rate of the AC edge is predicted to be faster than the ZZ, leading to the ZZ edge's dominating of the circumference of growing graphene islands. With the decrease in the temperature, the growth ratio of R/R_{ZZ} increases greatly, driving the AC edge to disappear quickly and leaving the pure ZZ geometry. This study presents reasonable grounds to understand relevant experimental observations. The information embodied in this work will not only help guide synthesis of the high-quality graphene but also control undesirable graphene formation in future experiments.

■ ASSOCIATED CONTENT

Supporting Information

K-point sampling test, Au/Ni adatom diffusion on the Ni(111) step, and reaction channel of the C pentamer production during C incorporation onto the AC graphene edge on the Ni(111) step. This material is available free of charge via the Internet at http://pubs.acs.org.

■ AUTHOR INFORMATION

Corresponding Author

*E-mail: huangyc@mail.ahnu.edu.cn.

Notes

The authors declare no competing financial interest.

■ ACKNOWLEDGMENTS

This work was supported by the National Younger Natural Science Foundation of China, No. 21203001, and the Natural Science Foundation of Anhui Province, No. 1208085QB37. Y. Huang thanks Dr. Prof. Z. X. Chen from Nanjing University for stimulating discussion.

■ REFERENCES

(1) Rümmeli, M. H.; Rocha, C. G.; Ortmann, F.; Ibrahim, I.; Sevincli, H.; Börrnert, F.; Kunstmann, J.; Bachmatiuk, A.; Pötschke, M.; Shiraishi, M.; Meyyappan, M.; Büchner, B.; Roche, S.; Cuniberti, G. *Adv. Mater.* **2011**, *23* (39), 4471−4490.

(2) Laosiripojana, N.; Assabumrungrat, S. *J. Power Sources* **2007**, *163* (2), 943−951.

(3) Comas, J.; Marino, F.; Laborde, M.; Amadeo, N. *Chem. Eng. J.* **2004**, *98* (1), 61−68.

(4) Novoselov, K. S.; Geim, A. K.; Morozov, S.; Jiang, D.; Zhang, Y.; Dubonos, S.; Grigorieva, I.; Firsov, A. *Science* **2004**, *306* (5696), 666−669.

(5) Sutter, P. *Nat. Mater.* **2009**, *8* (3), 171−172.

(6) Stankovich, S.; Dikin, D. A.; Piner, R. D.; Kohlhaas, K. A.; Kleinhammes, A.; Jia, Y.; Wu, Y.; Nguyen, S. T.; Ruoff, R. S. *Carbon* **2007**, *45* (7), 1558−1565.

(7) Coraux, J.; Engler, M.; Busse, C.; Wall, D.; Buckanie, N.; Zu Heringdorf, F.-J. M.; Van Gastel, R.; Poelsema, B.; Michely, T. *New J. Phys.* **2009**, *11* (2), 023006.

(8) Martinez-Galera, A. J.; Brihuega, I.; Gomez-Rodriguez, J. M. *Nano Lett.* **2011**, *11* (9), 3576−3580.

(9) Karoui, S.; Amara, H.; Bichara, C.; Ducastelle, F. *ACS Nano* **2010**, *4* (10), 6114−6120.

(10) Sutter, P. W.; Flege, J.-I.; Sutter, E. A. *Nat. Mater.* **2008**, *7* (5), 406−411.

(11) Reina, A.; Jia, X.; Ho, J.; Nezich, D.; Son, H.; Bulovic, V.; Dresselhaus, M. S.; Kong, J. *Nano Lett.* **2008**, *9* (1), 30−35.

(12) Li, X.; Cai, W.; An, J.; Kim, S.; Nah, J.; Yang, D.; Piner, R.; Velamakanni, A.; Jung, I.; Tutuc, E. *Science* **2009**, *324* (5932), 1312−1314.

(13) Kwon, S.-Y.; Ciobanu, C. V.; Petrova, V.; Shenoy, V. B.; Bareno, J.; Gambin, V.; Petrov, I.; Kodambaka, S. *Nano Lett.* **2009**, *9* (12), 3985−3990.

(14) Gao, J.; Yuan, Q.; Hu, H.; Zhao, J.; Ding, F. *J. Phys. Chem. C* **2011**, *115* (36), 17695−17703.

(15) Loginova, E.; Bartelt, N. C.; Feibelman, P. J.; McCarty, K. F. *New J. Phys.* **2008**, *10* (9), 093026.

(16) Chen, H.; Zhu, W.; Zhang, Z. *Phys. Rev. Lett.* **2010**, *104* (18), 186101.

(17) Meng, L.; Sun, Q.; Wang, J.; Ding, F. *J. Phys. Chem. C* **2012**, *116* (10), 6097−6102.

(18) Amara, H.; Bichara, C.; Ducastelle, F. *Phys. Rev. B* **2006**, *73* (11), 113404.

(19) Wang, Y.; Page, A. J.; Nishimoto, Y.; Qian, H.-J.; Morokuma, K.; Irle, S. *J. Am. Chem. Soc.* **2011**, *133* (46), 18837−18842.

(20) Koskinen, P.; Malola, S.; Hakkinen, H. *Phys. Rev. Lett.* **2008**, *101* (11), 115502.

(21) Yuan, Q.; Gao, J.; Shu, H.; Zhao, J.; Chen, X.; Ding, F. *J. Am. Chem. Soc.* **2011**, *134* (6), 2970−2975.

(22) Gomez-Gualdron, D. A.; Zhao, J.; Balbuena, P. B. *J. Chem. Phys.* **2011**, *134*, 014705.

(23) Ramirez-Caballero, G. E.; Burgos, J. C.; Balbuena, P. B. *J. Phys. Chem. C* **2009**, *113* (35), 15658−15666.

(24) Yazyev, O. V.; Pasquarello, A. *Phys. Rev. Lett.* **2008**, *100* (15), 156102.

(25) Shu, H.; Chen, X.; Tao, X.; Ding, F. *ACS Nano* **2012**, *6* (4), 3243−3250.

(26) Wang, L.; Zhang, X.; Chan, H. L.; Yan, F.; Ding, F. *J. Am. Chem. Soc.* **2013**, *135* (11), 4476−4482.

(27) Rostrup-Nielsen, J. R. *J. Catal.* **1984**, *85* (1), 31−43.

(28) Besenbacher, F.; Chorkendorff, I.; Clausen, B. S.; Hammer, B.; Molenbroek, A. M.; Norskov, J. K.; Stensgaard, I. *Science* **1998**, *279* (5358), 1913−1915.

(29) Rostrup-Nielsen, J. R.; Sehested, J.; Norskov, J. K. *Adv. Catal.* **2002**, *47*, 65−139.

(30) Bengaard, H. S.; Norskov, J. K.; Sehested, J.; Clausen, B. S.; Nielsen, L. P.; Molenbroek, A. M.; Rostrup-Nielsen, J. R. *J. Catal.* **2002**, *209* (2), 365−384.

(31) Arbag, H.; Yasyerli, S.; Yasyerli, N.; Dogu, G. *Int. J. Hydrogen Energy* **2010**, *35* (6), 2296−2304.

(32) Garcia-Dieguez, M.; Pieta, I. S.; Herrera, M. C.; Larrubia, M. A.; Alemany, L. J. *J. Catal.* **2010**, *270* (1), 136−145.

(33) Liu, C.; Ye, J.; Jiang, J.; Pan, Y. *ChemCatChem* **2011**, *3* (3), 529−541.

(34) Weatherup, R. S.; Bayer, B. C.; Blume, R.; Ducati, C.; Baehtz, C.; Schlogl, R.; Hofmann, S. *Nano Lett.* **2011**, *11* (10), 4154−4160.

(35) Liu, X.; Fu, L.; Liu, N.; Gao, T.; Zhang, Y.; Liao, L.; Liu, Z. *J. Phys. Chem. C* **2011**, *115* (24), 11976−11982.

(36) Chen, S.; Cai, W.; Piner, R. D.; Suk, J. W.; Wu, Y.; Ren, Y.; Kang, J.; Ruoff, R. S. *Nano Lett.* **2011**, *11* (9), 3519−3525.

(37) Dai, B.; Fu, L.; Zou, Z.; Wang, M.; Xu, H.; Wang, S.; Liu, Z. *Nat. Commun.* **2011**, *2*, 522.

(38) Kresse, G.; Furthmuller, J. *Phys. Rev. B* **1996**, *54* (16), 11169−11186.

(39) Kresse, G.; Furthmuller, J. *Comput. Mater. Sci.* **1996**, *6* (1), 15−50.

(40) Kresse, G.; Hafner, J. *Phys. Rev. B* **1993**, *47* (1), 558−561.

(41) Perdew, J. P.; Burke, K.; Ernzerhof, M. *Phys. Rev. Lett.* **1996**, *77* (18), 3865−3868.

(42) White, J.; Bird, D. *Phys. Rev. B* **1994**, *50* (7), 4954.

(43) Perdew, J. P.; Chevary, J.; Vosko, S.; Jackson, K. A.; Pederson, M. R.; Singh, D.; Fiolhais, C. *Phys. Rev. B* **1992**, *46* (11), 6671.

(44) Monkhorst, H. J.; Pack, J. D. *Phys. Rev. B* **1976**, *13* (12), 5188−5192.
(45) Methfessel, M.; Paxton, A. T. *Phys. Rev. B* **1989**, *40* (6), 3616.
(46) Henkelman, G.; Jonsson, H. *J. Chem. Phys.* **2000**, *113* (22), 9978−9985.
(47) Henkelman, G.; Uberuaga, B. P.; Jonsson, H. *J. Chem. Phys.* **2000**, *113* (22), 9901−9904.
(48) Gao, J.; Yip, J.; Zhao, J.; Yakobson, B. I.; Ding, F. *J. Am. Chem. Soc.* **2012**, *133* (13), 5009−5015.
(49) Luo, Z.; Kim, S.; Kawamoto, N.; Rappe, A. M.; Johnson, A. C. *ACS Nano* **2011**, *5* (11), 9154−9160.
(50) Sun, Q.; Yerino, C. D.; Leung, B.; Han, J.; Coltrin, M. E. *J. Appl. Phys.* **2011**, *110* (5), 053517−053517-10.
(51) Wu, P.; Zhang, W.; Li, Z.; Yang, J.; Hou, J. G. *J. Chem. Phys.* **2010**, *133*, 071101.
(52) Liu, Y.; Dobrinsky, A.; Yakobson, B. I. *Phys. Rev. Lett.* **2010**, *105* (23), 235502.